Semiconductor Physics, Quantum Electronics & Optoelectronics. 2001. V. 4, N 2. P. 118-122.

PACS: 61.10.E, 61.72.D

X-ray characterization of ZnSe single crystals doped with Mg

A.G. Fedorov, Yu.A. Zagoruiko, O.A. Fedorenko, N.O. Kovalenko

Institute for Single Crystals, National Academy of Sciences of Ukraine
60 Lenin Ave., 61001 Kharkiv, Ukraine

Abstract. Doping of cubic ZnSe with certain impurities like Mg or Mn during crystal growth causes the increased contents of the hexagonal phase in the crystal or even the transformation to hexagonal wurtzite modification that possess the anisothropy of properties. This opens the possibility to design not only the passive optical elements of this material but provide them with controlling or measuring functions. In the present work the structure evolution of ZnSe single crystals due to the Mg doping of different concentration was examined using the double crystal X-ray spectrometer.

Keywords: ZnSe, doping, structure, X-ray diffraction, twins.

Paper received 03.11.00; revised manuscript received 18.01.01; accepted for publication 16.02.01.

1. Introduction

From the point of its physical properties single crystalline ZnSe is one of the best choices for applications as IR optical elements. Low temperature modification of pure perfect zinc selenide has the cubic sphalerite structure with isotropic physical properties. But doping with certain impurities during ZnSe crystal growth leads to increased contents of the hexagonal phase in the crystal or transformation to hexagonal wurtzite modification that brings the anisothropy of properties. Arising birefringence allows to suggest the controlling or measuring applications for ZnSe construction elements. In present work the structure evolution of ZnSe single crystals due to the Mg doping of different concentration was examined using the double crystal X-ray spectrometer. ZnSe single crystal was grown from melt in argon ambient. Growth conditions provide the graded contents of Mg impurity from 2 to 7% measured with electron-probe microanalysis.

2. Background

The known peculiarity of $A^{II}B^{VI}$ crystals is the presence of stacking faults and twins lying in one of {111} planes. Density of these structure defects is dependent on the crystal growth conditions and, especially, on the contents of contaminations. To understand the influence of stacking faults and twins on the diffraction pattern, some theoretical considerations are necessary. X-ray scattering in the crystals liable to formation of stacking faults and twins was examined in wide range of publications. We shall use the conventional procedure based on the kinematical approach to construct the total scattered amplitude by summation on the elementary cells.

Pure perfect ZnSe crystal possess the cubic sphalerite structure. Planar defects disposed in (111) planes may be described as a shift of the next atomic plane for the case of stacking fault or rotation on 180° around <111> direction that creates the twin boundary between two parts of such crystal. As we consider the sequence of close packed planes in <111> direction and their shifts or rotations in (111) plane, it is suitable to make use of hexagonal cell with *a* and *b* axes lying in (111) cubic plane and *c* axis normal to it. Herein after cubic indices will be supplied with «*c*» sign and hexagonal with «*h*». Both cells are shown in Fig. 1. In a perfect crystal this hexagonal cell consists of three successive layers of type A and type B atoms and contains 3 pairs of A and B atoms per cell. But for the crystal containing stacking faults and twins disposed on arbitrary distances from one another, the unit cell of one interplanar distance height is more suitable. Thus, the summary scattered amplitude of perfect crystal is proportional to sum of phase shifts $G = \sum_n \exp in\delta$ where $\delta = 2\pi\left(\frac{h}{3} + \frac{2k}{3} + l\right)$ since follow-

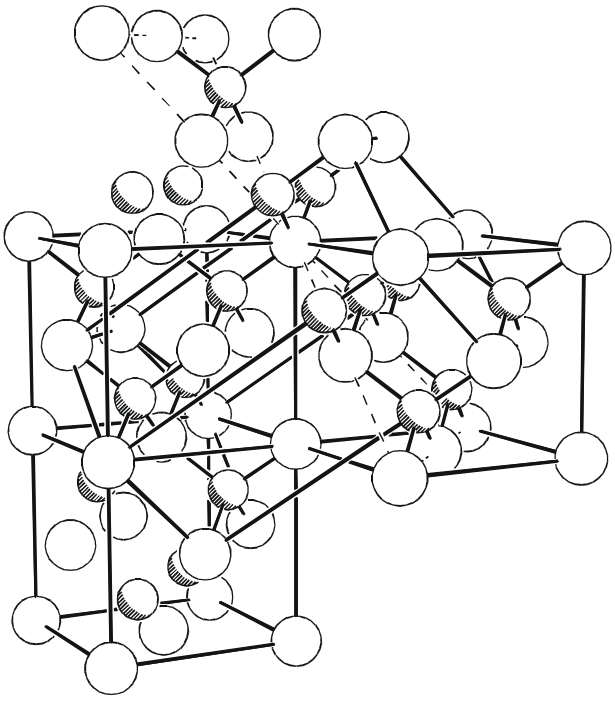

Fig. 1. Sphalerite lattice and transition to hexagonal cell.

ing layer in c direction is shifted on 1/3 and 2/3 of lattice periods along a and b axes relative to previous. Presence of the stacking fault causes additional shift along a and b. Supposing the most simple case of equidistant stacking faults, it may be shown easily that now

$$G = \sum_{m=0}^{t-1} \exp im\delta \sum_{n=0}^{N-1} \exp in(\varphi + t\delta) \text{ where } \varphi = 2\pi\left(\frac{h}{3} + \frac{k}{3}\right),$$

t is the quantity of layers between the stacking faults and N is the quantity of stacking faults in crystal. Here

$$\sum_{m=0}^{t-1} \exp im\delta$$

stands as a structure amplitude of the big unit cell with dimension dt along c axis, if d is the distance between layers along c.

Regarding the general case of randomly disposed stacking faults, one can obtain [1]

$$G = \frac{1}{1-\exp i\delta} \sum_{n=0} \exp in\varphi \exp iz_n\delta\,[1-\exp i\delta(z_{n+1}-z_n)] \tag{1}$$

Here n is the number of stacking fault, z_n – number of the plane where it appears.

Commonly probabilities of the stacking fault appearance in some distances are assumed and the average values of products of the complex conjugated amplitudes for their different pairs are derived [1–4]. Here another way is accepted. Direct expression is used for the summary phase shift on the structure with randomly distributed stacking faults or twin boundaries. Scattered intensity is proportional to the product of complex conjugated amplitudes. Distribution of defects with specified average distance and dispersion is created using the random number generator. So the resulting calculated picture of scattering is dependent on the following parameters: (a) average distance between defects and (b) dispersion of the distances.

Appointing $\bar{t}$ as the average distance between stacking faults, $z_n = n\bar{t} + \Delta t_n$, Δt_n is the deviation from average space for n-th stacking fault, (1) is transformed to

$$G = \frac{1}{1-\exp i\delta} \sum_{n=0} \exp in\varphi \exp i(n\bar{t} + \Delta t_n)\delta\{1-$$
$$-\exp i\delta[(n+1)\bar{t} + \Delta t_{n+1} - n\bar{t} - \Delta t_n]\} = \frac{1}{1-\exp i\delta} \times$$
$$\times \sum_{n=0} \exp in(\varphi + \delta\bar{t}) \exp i\Delta t_n\delta[1-\exp i\delta(\bar{t} + \Delta t_{n+1} - \Delta t_n)] \tag{2}$$

Multiplication of (2) to complex conjugated value yields

$$GG^* = \frac{1}{1-\cos\delta}\{\sum_{u=0}^{N-2} \sum_{v=u+1}^{N-1} \cos[(u-v)(\varphi+\delta\bar{t}) +$$
$$(\Delta t_u - \Delta t_v)\delta] - \cos[(u-v)(\varphi+\delta\bar{t}) +$$
$$+(\Delta t_u - \Delta t_{v+1} - \bar{t})\delta] - \cos[(u-v)(\varphi+\delta\bar{t}) +$$
$$+(\bar{t} + \Delta t_{u+1} - \Delta t_v)\delta] + \cos[(u-v)(\varphi+\delta\bar{t}) + \tag{3}$$
$$+(\Delta t_{u+1} - \Delta t_{v+1})\delta] + \sum_{u=0}^{N-1} 1 - \cos(\bar{t} + \Delta t_{u+1} - \Delta t_u)\delta\}$$

Passing across the twin boundary lying, say, between n+2 and n+3 layers gives the following consequence of phase shifts

$$\ldots \exp i(n\varphi + m\psi) + \exp i[(n+1)\varphi + (m+1)\psi] +$$
$$+\exp i[(n+2)\varphi + (m+2)\psi] + \exp i[(n+3)\varphi +$$
$$+(m+1)\psi] + + \exp i[(n+4)\varphi + m\psi] +$$
$$+\exp i[(n+5)\varphi + (m-1)\psi] + \ldots$$

that gives the 180° rotated or mirrorwise placed parts of structure; $\psi = 2\pi l$. In general, supposing sections of structure in initial orientation having t_1 thickness and opposite oriented sections (twins) with t_2 thickness, we get the sum

$$G = \left(\frac{1-\exp i\delta t_1}{1-\exp i\delta} + \frac{1-\exp i\gamma t_2}{1-\exp i\gamma} \exp i\delta t_1\right) \times$$
$$\times \sum_{n=0} (\exp i\delta t_1 \exp i\gamma t_2)^n \tag{4}$$

where $\delta = \varphi + \psi$, $\gamma = \psi - \varphi$ and intensity for this structure is proportional to

$$GG^* = \left[\frac{1-\cos\delta t_1}{1-\cos\delta} + \frac{1-\cos\gamma t_2}{1-\cos\gamma} - \right.$$
$$\left. - \frac{Y}{2(1-\cos\delta-\cos\gamma)+\cos 2\varphi+\cos 2\psi}\right]\times \qquad (5)$$
$$\times \frac{1-\cos N(\delta t_1+\gamma t_2)}{1-\cos(\delta t_1+\gamma t_2)}$$

where

$$Y = 1-\cos\delta t_1-\cos\gamma t_2+\cos(\delta t_1-\gamma)+\cos(\gamma t_2+\delta)+$$
$$+\cos\delta(t_1+1)+\cos\gamma(t_2-1)-\cos(\delta t_1+2\varphi)-$$
$$-\cos(\gamma t_2+2\varphi)+\cos(\delta t_1+\gamma t_2)-\cos(\delta t_1+\gamma t_2+\delta)-$$
$$-\cos(\delta t_1+\gamma t_2-\gamma)+\cos(\delta t_1+\gamma t_2+2\varphi)-$$
$$-\cos\delta-\cos\gamma+\cos 2\varphi$$

Eq. (5) is suitable to calculate diffraction on the structure containing ordered twins or polytypes. For example, putting $t_1 = t_2 = 3$ in (5) allows to simulate diffraction on 6H polytype; $t_1 = 3$ and $t_2 = 2$ corresponds to 15R one. If $t_1 = t_2 = 1$ then this is perfect hexagonal 2H lattice. Transformation of diffraction pattern calculated with Eq. (5) at transition from pure hexagonal 2H structure to twinned 3C sphalerite structure through polytypes of different magnitude is shown in Fig. 2. Reflection indices used of conventional wurtzite 2-layer cell and differ from accepted 3-layer hexagonal cell shown in Fig. 1 by factor of 2/3. The last curve in Fig. 2 denoted 100H represents the diffraction pattern for sphalerite containing large twinned blocks and consist of the set of usual cubic reflections and extra reflections that appears due to rotation twins. This known result is illustrated with projection of the reciprocal lattice shown on Fig. 3. It is evident from above that twins and polytypes may be detected examining the reciprocal space in directions set with $10l_h$, $20l_h$ nodes bearing in mind that both projections on $(\bar{1}10)_c$ and $(110)_c$ must be tested.

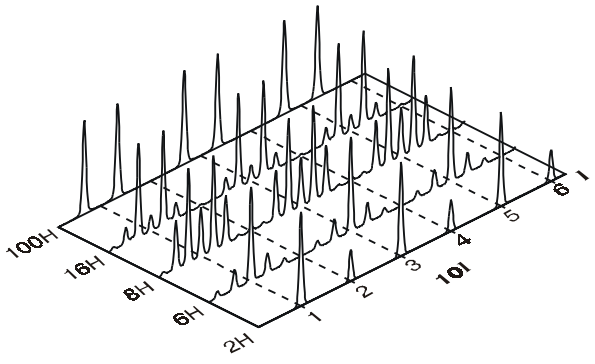

Fig. 2. Calculated set of $10l_h$ type reflections at transition from hexagonal 2H to sphalerite 3C twinned structure through polytypes of different magnitude.

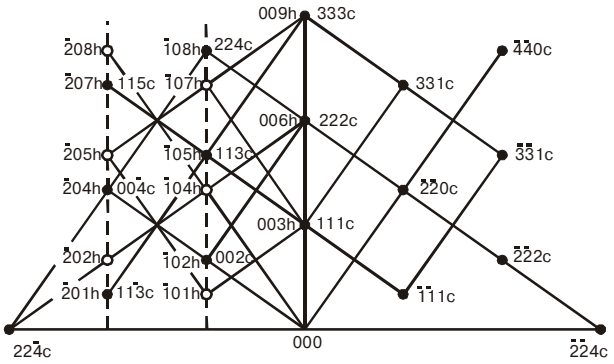

Fig. 3. Section of sphalerite reciprocal lattice by $(\bar{1}10)_c$ 1 plane. Conventionally perfect lattice is shown on the right half and twinned on the left half. Empty circles represent extra nodes.

In general case the expression for scattered amplitude at arbitrary distances between twin boundaries is desirable. In this work it was found directly in a same way for specified average value of inter-boundary distance and its dispersion. It is brought without cumbersome derivation.

$GG^* = S_1 + S_2 + S_3$, where

$$S_1 = \frac{1}{1-\cos\delta}\left[\frac{N}{2} - \sum_{j=0}^{\frac{N}{2}-1}\cos\delta t_{2j} + \sum_{u=0}^{\frac{N}{2}-2}\sum_{v=u+1}^{\frac{N}{2}-1}\cos(a+b_1) - \right.$$
$$\left. - \cos(a+b_2) - \cos(a+b_3) + \cos(a+b_4)\right]$$
$$a = \gamma\sum_{j=u}^{v-1} t_{2j+1} \quad b_1 = \delta\sum_{j=u}^{v-1} t_{2j} \quad b_2 = \delta\sum_{j=u+1}^{v-1} t_{2j} \quad b_3 =$$
$$= \delta\sum_{j=u}^{v} t_{2j} \quad b_4 = \delta\sum_{j=u+1}^{v} t_{2j}$$

with condition: if $v = u+1$ then $b_2 = 0$;

$$S_2 = \frac{1}{1-\cos\gamma}\left[\frac{N}{2} - \sum_{j=0}^{\frac{N}{2}-1}\cos\gamma t_{2j+1} + \sum_{u=0}^{\frac{N}{2}-2}\sum_{v=u+1}^{\frac{N}{2}-1}\cos(c+d_1) - \right.$$
$$\left. - \cos(c+d_2) - \cos(c+d_3) + \cos(c+d_4)\right]$$
$$c = \delta\sum_{j=u+1}^{v} t_{2j} \quad d_1 = \gamma\sum_{j=u}^{v-1} t_{2j+1} \quad d_2 = \gamma\sum_{j=u+1}^{v-1} t_{2j+1} \quad d_3 =$$
$$= \gamma\sum_{j=u}^{v} t_{2j+1} \quad d_4 = \gamma\sum_{j=u+1}^{v} t_{2j+1}$$

with condition: if $v = u+1$ then $d_2 = 0$;

$$S_3 = \frac{1}{2(1-\cos\gamma-\cos\delta)+\cos 2\varphi+\cos 2\psi}\times$$
$$[\sum_{u=0}^{\frac{N}{2}-1}\sum_{v=u}^{\frac{N}{2}-1}\cos(e_1+f_1)-\cos(e_1+f_2)-\cos(e_2+f_1)+$$
$$+\cos(e_2+f_2)-\cos(e_1+f_1-\gamma)+\cos(e_1+f_2-\gamma)+$$
$$+\cos(e_2+f_1-\gamma)-\cos(e_2+f_2-\gamma)-\cos(e_1+f_1+\delta)+$$
$$+\cos(e_1+f_2+\delta)+\cos(e_2+f_1+\delta)-\cos(e_2+f_2+\delta)+$$
$$+\cos(e_1+f_1+2\varphi)-\cos(e_1+f_2+2\varphi)-$$
$$-\cos(e_2+f_1+2\varphi)+\cos(e_2+f_2+2\varphi)]$$
$$e_1=\delta\sum_{j=u}^{v}t_{2j}\quad e_2=\delta\sum_{j=u+1}^{v}t_{2j}$$
$$f_1=\gamma\sum_{j=u}^{v-1}t_{2j+1}\quad f_2=\gamma\sum_{j=u}^{v}t_{2j+1} \qquad (6)$$

with condition: if $u=v$ then $e_2 = 0, f_1 = 0$.

Last expression looks something bulky but advantaged with easy programming.

Thus the expressions obtained allow to simulate diffraction on the $A^{II}B^{VI}$ structure containing arbitrary disposed stacking faults – Eg. (3), polytypes – Eg. (5) and twins on arbitrary distances – Eg. (6). Of course, equations for twins are more general, it is possible to calculate diffraction on the structure with stacking faults using (5) or (6) assigning the unit thickness for each alternate twin.

3. Experimental

For X-ray investigations the specimens of about 0.5 mm dimension were picked from the parts of ZnSe crystal with different contents of Mg. The reciprocal space of the specimens was inspected searching $10l_h$ or $20l_h$ reflections in both projections mentioned above. Since the disposition of twins is connected with the direction of crystal growth, twin extra reflections appeared only in one of two orientations. The extra reflections confirming the presence of twins were detected in all specimens of this example of ZnSe crystal. Diffraction patterns of the specimens with Mg concentration below about 3.5% exhibit very weak additional peaks that appears between main and extra reflections. Simulations show that it corresponds to twins more than 60 layers thick and picture depends appreciably from the dispersion of twins dimensions. Diffraction pattern for the specimen with 2.5% Mg contents is shown in Fig. 4. Increase of Mg concentration to 4.5% leads to changes in diffraction pattern as shown in Fig. 5. Numerical simulation prove the increased extent of ordering and smaller thickness of twins. The most remarkable effect of Mg doping was observed at approximately 6.1% impurity concentration. Reflections inherent to sphalerite lattice entirely disappeared and diffraction pattern becomes conformable to the hexagonal lattice with doubled period in *c* axis direction. Calculation shows a good agreement with diffraction on 4H polytype (Fig. 6). Further increase of Mg concentra-

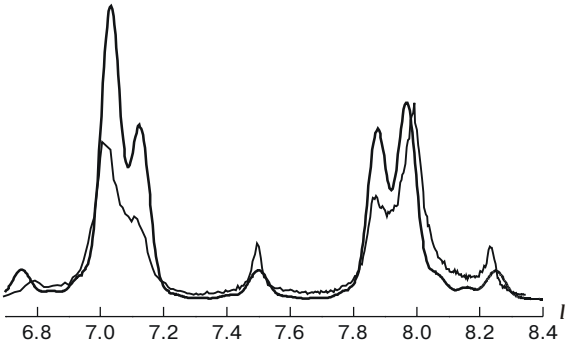

Fig. 5. Experimental diffraction pattern (20*l*)h for 4.5% Mg containing specimen (thin) and calculated pattern for 16 - layer twins (bold).

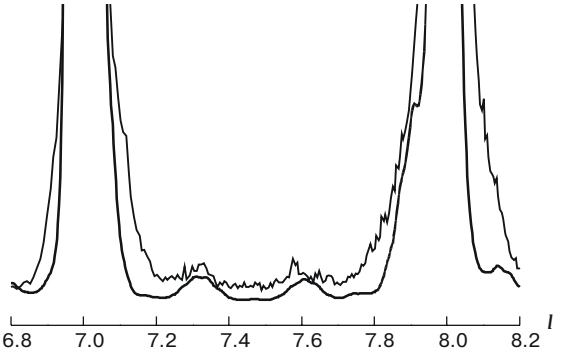

Fig. 4. Experimental diffraction pattern (10*l*)h for 2.5% Mg containing specimen (thin) and calculated one for 90 - layer twins (bold).

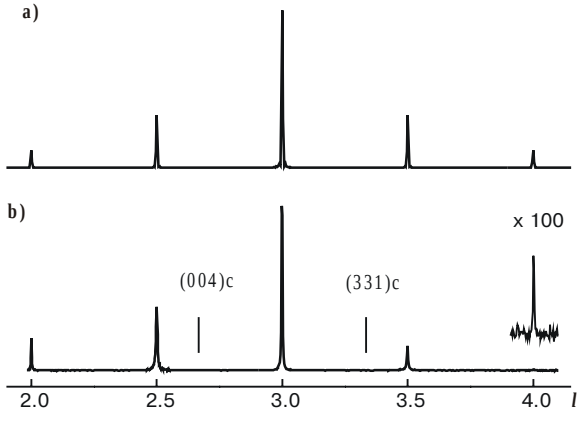

Fig. 6. Calculated pattern for 4H polytype (a) and experimental (20*l*)h diffraction pattern for the specimen with 6.1% Mg concentration (b). Indexes *l* corresponds to conventional hexagonal lattice 2H. Strokes show positions of disappeared cubic reflections.

tion leads to disappearance of such good ordering. Diffraction shows only remaining large twins and development of the block crystal structure.

Conclusions

It was shown that crystalline structure of ZnSe single crystal is very sensitive to the Mg doping in the range 3 to 6%. Initial sphalerite lattice with comparatively large twinned blocks gains more ordered and thin twins and becomes closer to polytype modification simultaneously with Mg concentration increase. The most pronounced effect of Mg doping was observed at approximately 6% of Mg. It was expressed in the emergence of well-ordered hexagonal structure with doubled elementary cell in *c* direction that corresponds to 4H polytype.

References

1. A.I.Ustinov, X-ray diffraction on 2H-crystals containing subtraction stacking faults of I_2 type // *Metallofizika* **9**(1), pp. 77-83 (1987) [in Russian].
2. A.J.C.Wilson, *X-ray optics*, London (1949).
3. M.Cesari and G.Allegra, The Intensity of X-rays Diffracted by Monodimensionally Disordered Structures // *Acta Crystallographica* **23**(2), pp. 200-205 (1967).
4. A.Yamamoto, Application of Modulated Structure Analysis to Polytypes // *Acta Crystallographica* **A37**(6), pp. 838-842 (1981).